Computer Physics Communications 182 (2011) 1767–1770

Contents lists available at ScienceDirect

Computer Physics Communications

www.elsevier.com/locate/cpc

Advanced physics calculations using a multi-fluid plasma model

U. Shumlak *, R. Lilly, N. Reddell, E. Sousa, B. Srinivasan

Aerospace and Energetics Research Program, University of Washington, Seattle, WA 98195-2250, USA

ARTICLE INFO

Article history:
Received 1 August 2010
Received in revised form 29 November 2010
Accepted 30 December 2010
Available online 5 January 2011

Keywords:
Multi-fluid plasma
Two-fluid equilibrium
Discontinuous Galerkin
Drift turbulence
Physics-based semi-implicit

ABSTRACT

The multi-fluid plasma model is derived from moments of the Boltzmann equation and typically has two fluids representing electron and ion species. Large mass differences between electrons and ions introduce disparate temporal and spatial scales and require a numerical algorithm with sufficient accuracy to capture the multiple scales. Source terms of the multi-fluid plasma model couple the fluids to themselves (interspecies interactions) and to the electromagnetic fields. The numerical algorithm must treat the inherent stiffness introduced by the multiple physical effects of the model and tightly couple the source terms of the governing equations. A discontinuous Galerkin method is implemented for the spatial representation. Time integration is investigated using explicit, implicit, semi-implicit methods. Semi-implicit treatment is accomplished using a physics-based splitting. The algorithm is applied to study drift turbulence in field reversed configuration plasmas to illustrate the physical accuracy of the model. The algorithm is also applied to plasma sheath formation which demonstrates Langmuir wave propagation.

1. Introduction

Understanding and predictability of plasma behavior has been significantly advanced through the development of reduced plasma models and their numerical solution. The most common reduced plasma model is the magnetohydrodynamic (MHD) model, which describes the plasma as a single-fluid. While the MHD model has been successful in many applications [1–4], more complex effects require more complete physical models. The most complete continuum model for plasma is described using kinetic theory where each species α of a plasma is described by a time-dependent distribution function $f_\alpha(\mathbf{x}, \mathbf{v}, t)$ in physical and velocity space. The evolution of the distribution functions is described by the Boltzmann equation

$$\frac{\partial f_\alpha}{\partial t} + \mathbf{v} \cdot \frac{\partial f_\alpha}{\partial \mathbf{x}} + \frac{q_\alpha}{m_\alpha}(\mathbf{E} + \mathbf{v} \times \mathbf{B}) \cdot \frac{\partial f_\alpha}{\partial \mathbf{v}} = \left.\frac{\partial f_\alpha}{\partial t}\right|_c . \tag{1}$$

The plasma is typically composed of ion and electron species and possibly additional species for neutrals or impurities. The Boltzmann equation coupled with Maxwell's equations for electromagnetic fields completely describe the plasma dynamics. Plasmas have been simulated using this model with specific forms of the collision operator (Vlasov equation and Fokker–Planck equation) [5–8]. However, the Boltzmann equation is seven-dimensional. As a consequence of the large dimensionality, plasmas are simulated using the Boltzmann equation only when necessary to capture the essential physics.

Another approach to capture more complete physics is to generalize the single-fluid MHD model. The generalization described here allows for multiple species — the multi-fluid plasma model. Each fluid is assumed to have a Maxwellian velocity distribution. The generalization also allows for atomic reactions such as ionization, recombination, and charge exchange. The analytical development of the model is briefly described in Section 2. Section 3 presents the numerical implementation and some of its features that are specifically important to the multi-fluid plasma model. Illustrative applications of the multi-fluid plasma model are presented in Section 4.

2. Multi-fluid plasma model

Taking moments of the Boltzmann equation, Eq. (1), provides equations that govern the evolution of the moment variables. The moment variables are defined from moments of the distribution function. The governing equations for the limiting case without atomic reactions and for a two-fluid (ions and electrons) plasma model is presented in Ref. [9].

The governing equations of the two-fluid plasma model can be combined to form the single-fluid MHD model [10]. In the derivation of the MHD model several approximations are made which limit its applicability to low frequency phenomena and ignores potentially significant finite electron mass and charge separation effects.

Generalizing the moment approach to include an arbitrary number of species and to include atomic reactions yields the multi-fluid plasma model. The derivation follows that provided by Braginskii in Ref. [11]. However, the form of the equations are derived here for the conservation variables in flux/source form where

* Corresponding author.
E-mail address: shumlak@u.washington.edu (U. Shumlak).

0010-4655/$ – see front matter
doi:10.1016/j.cpc.2010.12.048

hyperbolic and parabolic fluxes are in balance with source terms. For example, the governing equations for the electron fluid are

$$\frac{\partial n_e}{\partial t} + \nabla \cdot (n_e \mathbf{v}_e) = \Gamma_{ion} - \Gamma_{rec}, \tag{2}$$

$$\frac{\partial}{\partial t}(\rho_e \mathbf{v}_e) + \nabla \cdot (\rho_e \mathbf{v}_e \mathbf{v}_e + \mathbb{P}_e) = -en_e(\mathbf{E} + \mathbf{v}_e \times \mathbf{B}) - \mathbf{R}_{ei} + \mathbf{R}_{ne} + m_e \mathbf{v}_n \Gamma_{ion} - m_e \mathbf{v}_e \Gamma_{rec}, \tag{3}$$

$$\frac{\partial \varepsilon_e}{\partial t} + \nabla \cdot (\varepsilon_e \mathbf{v}_e + \mathbf{v}_e \cdot \mathbb{P}_e + \mathbf{h}_e) = -\mathbf{v}_e \cdot (en_e \mathbf{E} + \mathbf{R}_{ei} - \mathbf{R}_{ne}) + Q_{ei} + Q_{en} + \left(\frac{1}{2} m_e v_n^2 - \phi_{ion}\right)\Gamma_{ion} - \frac{1}{2} m_e v_e^2 \Gamma_{rec}, \tag{4}$$

where the conservation variables are number density $n_e = \rho_e/m_e$, momentum density $\rho_e \mathbf{v}_e$, and total energy density ε_e. The total energy density is defined as the sum of the internal energy and kinetic energy.

$$\varepsilon_e \equiv \frac{3}{2} n_e T_e + \frac{1}{2} \rho_e v_e^2, \tag{5}$$

and the electron temperature T_e is defined by the scalar electron pressure p_e from the second moment of the distribution function,

$$n_e T_e = p_e \equiv \frac{1}{3} \int m_e w^2 f_e \, d\mathbf{v}, \tag{6}$$

where $w = |\mathbf{v}_e - \mathbf{v}|$ is the random velocity of the electron species. The electron pressure tensor $\mathbb{P}_e$ can deviate from the scalar electron pressure. Closure statements are required to relate these terms to the other variables in the system [11]. The heat flux $\mathbf{h}_e$ is defined by a closure statement that relates it to the temperature gradient, i.e. $\mathbf{h}_e \propto \nabla T_e$. Collisional effects originate from the right hand side of Eq. (1) and provide a mechanism for momentum transfer, e.g. $\mathbf{R}_{ei}$, and a mechanism for heat generation, e.g. Q_{ei}. The atomic reaction rates are given by Γ_{ion} and Γ_{rec} for ionization and recombination which include the charge exchange reaction. Governing equations similar to Eqs. (2)–(4) exist for each ionic species and each neutral species. (Neutral species do not experience forces directly from the electric and magnetic fields.) The five moment equations given by Eqs. (2)–(4) are sufficient for describing the evolution of an electron fluid in thermodynamic equilibrium. The distribution function for the electrons f_e is described by a Maxwellian distribution. Provided the other fluids are each in thermodynamic equilibrium, similar five moment equations are sufficient to describe their evolution. Equal temperatures are not required, e.g. $T_e \neq T_i \neq \cdots$.

The electric and magnetic fields, **E** and **B**, appear in the source terms of the fluid equations, e.g. the Lorentz force in Eq. (3). The field dynamics are governed by Maxwell's equations, which have source terms that contain the fluid variables. For example, Ampere's law and Gauss's law are expressed as

$$\epsilon_0 \mu_0 \frac{\partial \mathbf{E}}{\partial t} - \nabla \times \mathbf{B} = -\mu_0 \sum_\alpha q_\alpha n_\alpha \mathbf{v}_\alpha, \tag{7}$$

$$\epsilon_0 \nabla \cdot \mathbf{E} = \sum_\alpha q_\alpha n_\alpha. \tag{8}$$

The motion of the plasma influences the evolution of the electromagnetic fields through the redistribution of charge density and current density.

The divergence constraints of Maxwell's equations can be difficult to satisfy with the presence of current and charge sources on an arbitrary computational grid. Maxwell's equations can be reformulated into a "purely hyperbolic" form (hyperbolic fluxes and source terms) by introducing two scalar correction potentials [12].

The multi-fluid plasma model is described by the equation system comprised of fluid equations for each species, appropriate closure statements and Maxwell's equations for the fields. As seen in the equation system, the fluids and fields are coupled through the source terms. Accurate calculation of the source terms and hyperbolic fluxes is particularly critical for steady-state equilibrium problems where large magnetic, electric, and pressure forces balance.

3. Numerical implementation

The governing equations for the multi-fluid plasma model (including the electromagnetic equations) are formulated in flux/source form as shown above. The entire equation system can be expressed in compact form as

$$\frac{\partial q}{\partial t} + \nabla \cdot \mathbf{F} = S, \tag{9}$$

where q is the vector of conserved variables, $\mathbf{F}$ is the tensor of hyperbolic fluxes, and S is the vector containing the source terms. The numerical implementation of the multi-fluid plasma model must provide an accurate and consistent treatment of the source terms and hyperbolic fluxes.

The spatial representation is accomplished with a high-order discontinuous Galerkin (DG) method [13–16]. The DG implementation is an unsplit method. Both the hyperbolic fluxes and source terms are represented with a high-order spatial representation and are integrated in time simultaneously. Split methods can lead to inaccurate balancing of the source terms and hyperbolic fluxes. Time-integration is accomplished using either an explicit TVD Runge–Kutta method, a fully implicit method, or a physics-based semi-implicit method.

3.1. Spatial representation — discontinuous Galerkin

The simulation domain is divided into discrete elements which are quadrilaterals in 2D and hexahedrals in 3D. The spatial variation of the conservation variables within each element is modeled by projecting the variables onto a set of basis functions v_h of order h, such that $q = \sum_h q_h v_h$. The basis functions are Legendre polynomials for the implementation described here. The governing equations are multiplied by each basis function and integrated over the element volume. An integral equation is generated for each basis function.

$$\int_\Omega v_h \frac{\partial q}{\partial t} dV + \oint_{\partial\Omega} v_h \mathbf{F} \cdot d\mathbf{S} - \int_\Omega \mathbf{F} \cdot \nabla v_h \, dV = \int_\Omega v_h S \, dV, \tag{10}$$

where the divergence theorem has been applied to the second term of Eq. (9). The volume and surface integrals are evaluated by Gaussian quadrature. The source terms are projected onto the basis functions and are, therefore, the same order accurate as the solution variables. This satisfies the high-order accuracy requirement to preserve the equilibrium balance between the divergence of the hyperbolic fluxes and the source terms. The hyperbolic fluxes at the element surfaces for the surface integral in Eq. (10) are calculated with a Roe-type approximate Riemann solver [9].

Spatial representations using up to 16th-order polynomials have been used. Such high orders are important for equilibrium problems.

3.2. Time integration — explicit, implicit, and semi-implicit

Several time-integration methods have been investigated. An explicit third-order TVD Runge–Kutta method has been implemented and works well provided the stability restriction is obeyed.

The CFL number must be less than 1/5 [17]. However, the multi-fluid plasma model allows for the propagation of waves that have disparate characteristic speeds. The speeds range from high speed of light ($\approx 10^8$ m/s) to slow speed of bulk fluid motion (≈ 1 m/s). Many simulations aim to study the plasma evolution over long timescales — many fluid transit times. Explicit simulations are thus computationally intensive.

Implicit methods allow for time steps that are not limited by the fast waves. The entire system of governing equations, Eq. (9), is written as

$$\frac{\partial q}{\partial t} = f(q). \tag{11}$$

The time advance can be expressed in an implicit form of arbitrary order accuracy. A second-order Crank–Nicolson method has been implemented, which is solved iteratively using a variety of implicit numerical methods.

The implicit method has been applied to several benchmark problems to compare the accuracy of the solution when large time steps are used. Solution accuracy is well preserved for the resolved timescale. However, formulating the implicit time-advance method for the multi-fluid plasma model results in a large, stiff equation system with a matrix that is difficult to invert. The multi-fluid plasma model contains 18 variables for the ion and electron fluids and the electromagnetic fields. Each additional fluid requires an additional 5 variables. None of the numerical methods, e.g. ILU preconditioned GMRES, have performed adequately without artificially altering the physics of the problem, like using unrealistically massive electrons with $m_i/m_e = 25$ [18].

A semi-implicit method has been formulated to perform a splitting of the governing equations based on the different expected physics and scales. The electron fluid and electromagnetic fields introduce the fast/small scales, and their governing equations are solved implicitly. The ion and neutral fluids introduce slow/large scales, and their governing equations are solved explicitly. The combination of implicit and explicit treatments limits the size of the operator matrix that needs inverting. The time step is still limited by the ion motion, which is often the timescale of interest.

4. Illustrative applications

The numerical algorithm described above has been implemented on parallel computers in a code named WARPX (Washington Approximate Riemann Plasma) for 2D and 3D for general geometries. The code has been benchmarked against several analytical and published computational problems [9,19,20].

4.1. Drift turbulence in FRC plasmas

The resulting numerical method has been applied to study Z-pinch dynamics [21,18] and three-dimensional field reversed configuration (FRC) evolution to investigate anomalous resistivity [20, 18] that experimentally limits the plasma current. FRCs form a toroidal equilibrium structure where a toroidal electron current is driven to create a poloidal magnetic field superimposed onto an external solenoidal magnetic field. The electron motion interacts with the magnetic field to confine an electron pressure. The confined electron fluid creates a radial electric field to confine the ion pressure. FRC plasma simulations require at least two fluids for accuracy.

Fig. 1 shows a sample evolution of an FRC plasma. The simulation is performed with $m_i/m_e = 25$, $c/v_A = 39$, and kinetic parameter $s = 7$. The corresponding time steps are 6×10^{-12}, 1×10^{-9}, and 6×10^{-7} s, for explicit, semi-implicit, and implicit methods. The FRC problem demonstrates the accurate balance of the hyperbolic fluxes and the source terms. Split methods cause the equilibrium to artificially dissipate. The simulation results in Fig. 1 demonstrate that equilibrium is maintained. The simulation also shows a drift turbulence instability develops in the toroidal direction. This instability may be related to anomalous resistivity observed in experiments.

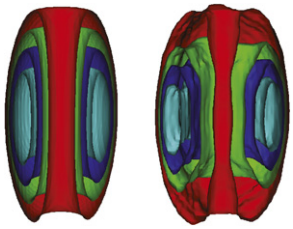

Fig. 1. Three-dimensional evolution of an FRC using the two-fluid WARPX code. Shown are ion density isosurfaces (1.8, 2.8, 3.8, 4.8×10^{-21} m^{-3}) for initial condition and after instability evolves. Electron density and pressures have a similar structure. Equilibrium is maintained. Small scale variations related to drift turbulence are evident in the toroidal direction.

4.2. Plasma sheath formation

A three-fluid (electrons, ions, and neutrals) simulation of plasma sheath formation is performed to illustrate the multi-fluid capability of the numerical algorithm. The sheath formation is studied by initializing uniform static fluids and no bias electric field. The boundaries are modeled with interleaved regions of dielectric and electrode materials. Electrical potentials can be applied to the electrodes. The simulation is performed with $m_i/m_e = 100$, $c/v_{Te} = 10$. Atomic reactions are incorporated that describe the effects of collisions between the species explicitly, allowing for the identification of regions of ionization/recombination and inter-species momentum and energy transfer. Plasma sheath formation is important for electrode-based plasma technologies, e.g. plasma actuators for control of high-speed aerospace vehicles. The multi-fluid model captures electron inertial effects and has revealed a physical effect not observed with other plasma models. During the initial formation of the plasma sheath, the applied electrode potential excites a Langmuir wave that propagates into the bulk plasma. The dispersion relation for the Langmuir wave is given by

$$\omega^2 = \omega_{pe}^2 + 1.5k^2 v_{Te}^2 \tag{12}$$

where ω_{pe} is the electron plasma frequency and v_{Te} is the electron thermal speed. Typically, sheath simulations assume electrostatic fields and miss the electrodynamics of the formation process [22]. Propagating Langmuir waves are shown in simulation results in Fig. 2, where parallel electrodes at ground potential are modeled to allow validation with theoretical predictions, such as the ions reach the Bohm velocity prior to the sheath edge. The numerical dispersion agrees with the relation of Eq. (12), as seen in Fig. 2.

The plasma sheath formation studies provide better physical understanding of the plasma production process. Plasma (ions and electrons) is produced by ionizing the neutral gas, and plasma is lost when it reaches the electrode and recombines. An analytical model of the electrode describes secondary electron emission and recombination at the electrode. In addition to the plasma sheath that naturally forms around electrodes, a voltage can be applied to the electrodes to drive a net current through the plasma. While steady-state cathode and anode drops are well understood analytically in simple geometries, the numerical solution of the multi-fluid plasma model with WARPX captures the details of the formation dynamics and allows for arbitrarily complex geometries and time-dependent phenomena.

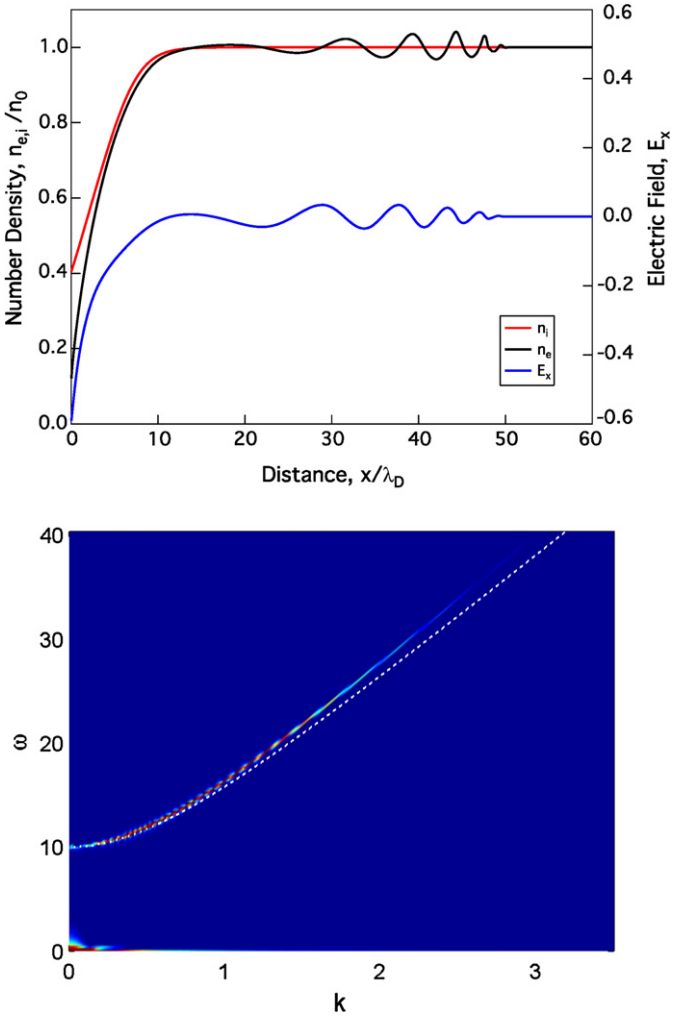

Fig. 2. Initial plasma production showing the propagation of a Langmuir wave in the electron density (black) and electric field (blue). The lower plot shows amplitude contours when the numerical results are Fourier transformed into wave space (k, ω). The numerical dispersion agrees well with analytical dispersion relation (white dotted line). (For interpretation of the references to color in this figure, the reader is referred to the web version of this article.)

5. Conclusions

The multi-fluid plasma model in flux/source form has been derived from moments of the Boltzmann equation combined with Maxwell's equations. The model captures more complete physics than the single-fluid MHD model. Accurate treatments of the source terms and hyperbolic fluxes are important since the fluids and fields are coupled through the source terms. A high-order discontinuous Galerkin method provides the necessary coupling and high spatial accuracy. A full implicit time integration implementation leads to an inefficient method since the large system size and disparate characteristic speeds result in a matrix that is difficult to invert. A physics-based, semi-implicit method splits the governing equations into two systems — one with fast characteristic speeds, which is integrated implicitly, and one with slow characteristic speeds, which is integrated explicitly. The numerical algorithm has been benchmarked and is producing physically-relevant simulations, such as FRC simulations of anomalous resistivity and plasma sheath formation.

Acknowledgements

This work is supported by a grant from the United States Air Force Office of Scientific Research.

References

[1] O.S. Jones, U. Shumlak, D.S. Eberhardt, An implicit scheme for nonideal magnetohydrodynamics, Journal of Computational Physics 130 (2) (1997) 231–242.
[2] S. Fromang, J. Papaloizou, MHD simulations of the magnetorotational instability in a shearing box with zero net flux, Astronomy and Astrophysics 476 (3) (2007) 1113–1122.
[3] V.A. Izzo, D.G. Whyte, R.S. Granetz, P.B. Parks, E.M. Hollmann, L.L. Lao, J.C. Wesley, Magnetohydrodynamic simulations of massive gas injection into Alcator C-Mod and DIII-D plasmas, Physics of Plasmas 15 (5) (2008).
[4] M. Selwa, S.K. Solanki, K. Murawski, T.J. Wang, U. Shumlak, Numerical simulations of impulsively generated vertical oscillations in a solar coronal arcade loop, Astronomy and Astrophysics 454 (2006) 653–661.
[5] C.Z. Cheng, G. Knorr, Integration of Vlasov equation in configuration space, Journal of Computational Physics 22 (3) (1976) 330–351.
[6] L. Chacon, D.C. Barnes, D.A. Knoll, G.H. Miley, An implicit energy-conservative 2D Fokker–Planck algorithm, Journal of Computational Physics 157 (2) (2000) 618–653.
[7] Y. Matsunaga, T. Hatori, T. Kato, Kinetic simulation of nonlinear phenomena of an ion acoustic wave in gas discharge plasma with convective scheme, Physics of Plasmas 8 (3) (2001) 1057–1069.
[8] M.H.L. van der Velden, W.J.M. Brok, J.J.A.M. van der Mullen, V. Banine, Kinetic simulation of an extreme ultraviolet radiation driven plasma near a multilayer mirror, Journal of Applied Physics 100 (7) (2006).
[9] U. Shumlak, J. Loverich, Approximate Riemann solver for the two-fluid plasma model, Journal of Computational Physics 187 (2) (2003) 620–638.
[10] Jeffrey P. Freidberg, Ideal Magnetohydrodynamics, Plenum Press, New York, London, 1987.
[11] S.I. Braginskii, Transport processes in a plasma, in: M.A. Leontovich (Ed.), Reviews of Plasma Physics, vol. 1, Consultants Bureau, New York, NY, 1965, pp. 205–311.
[12] C.D. Munz, P. Ommes, R. Schneider, A three-dimensional finite volume solver for the Maxwell equations with divergence cleaning on unstructured meshes, Computer Physics Communications 130 (2000) 83–117.
[13] B. Cockburn, C.W. Shu, TVB Runge–Kutta local projection discontinuous Galerkin finite-element method for conservation-laws, Mathematics of Computation 52 (186) (1989) 411–435.
[14] B. Cockburn, S.C. Hou, C.W. Shu, The Runge–Kutta local projection discontinuous Galerkin finite-element method for conservation-laws, Mathematics of Computation 54 (190) (1990) 545–581.
[15] B. Cockburn, C.W. Shu, The Runge–Kutta discontinuous Galerkin method for conservation-laws, Journal of Computational Physics 141 (2) (1998) 199–224.
[16] J. Loverich, U. Shumlak, A discontinuous Galerkin method for the full two-fluid plasma model, Computer Physics Communications 169 (1–3) (2005) 251–255.
[17] B. Cockburn, C.W. Shu, Runge–Kutta discontinuous Galerkin methods for convection-dominated problems, Journal of Scientific Computing 16 (3) (2001) 173–261.
[18] B. Srinivasan, Numerical methods for 3-dimensional magnetic confinement configurations using two-fluid plasma equations, PhD thesis, University of Washington, Seattle, WA 98195, June 2010.
[19] A. Hakim, J. Loverich, U. Shumlak, A high resolution wave propagation scheme for ideal two-fluid plasma equations, Journal of Computational Physics 219 (1) (2006) 418–442.
[20] A. Hakim, U. Shumlak, Two-fluid physics and field-reversed configurations, Physics of Plasmas 14 (5) (2007) 055911.
[21] J. Loverich, U. Shumlak, Nonlinear full two-fluid study of $m = 0$ sausage instabilities in an axisymmetric Z pinch, Physics of Plasmas 13 (8) (2006) 082310.
[22] S. Roy, B.P. Pandey, J. Poggie, D.V. Gaitonde, Modeling low pressure collisional plasma sheath with space-charge effect, Physics of Plasmas 10 (6) (2003) 2578–2585.